Vol. 744: 69–82, 2024
https://doi.org/10.3354/meps14668

MARINE ECOLOGY PROGRESS SERIES
Mar Ecol Prog Ser

Published September 5

Activity of the shallow-water hydrothermal vent crab *Xenograpsus testudinatus* is affected by tides, water temperature, and light intensity

Benny K. K. Chan[1], Jyun-Cheng Guo[2], Chien-Lin Chen[2], Tin-Yam Chan[2,3,*]

[1]Biodiversity Research Center, Academia Sinica, Taipei 115, Taiwan, ROC
[2]Institute of Marine Biology, National Taiwan Ocean University, Keelung 20224, Taiwan, ROC
[3]Center of Excellence for the Oceans, National Taiwan Ocean University, Keelung 20224, Taiwan, ROC

ABSTRACT: The activity pattern of the shallow-water hydrothermal vent crab *Xenograpsus testudinatus* in the vent and peripheral regions of Kueishan Island, Taiwan, was observed using an underwater time-lapse camera with infrared lighting during 7 consecutive 2–3 d periods. Hourly tide levels, *in situ* water temperature, pH, and light intensity were recorded to examine any effects of these environmental factors on crab activity. Time series analysis using spectral density plots indicated that crab activities were not rhythmic. Nevertheless, cross-correlation analysis and Pearson's correlation showed that crab density in the vent region was negatively correlated with tide but positively correlated with water temperature and light intensity. Stepwise multiple regression analysis showed that water temperature, tide levels, and light intensity are significant predictors of crab density. There were no significant differences in crab density among specific tide periods, and thus, a previous hypothesis that vent crabs emerge in large swarms during slack waters was rejected. The vent region is a refuge from predators, with crabs more active during daytime low tides and during periods with higher water temperatures. Crab density in the peripheral region is positively correlated with tide but negatively correlated with pH, indicating that crabs there are more active at high tides while foraging and during periods with lower pH, probably when there are fewer predators. Stepwise multiple regression revealed pH and tides were significant predictors for crab density in the peripheral region.

KEY WORDS: Crustacea · Brachyura · Diurnal activity · Behavior · Underwater monitoring · Infrared

Resale or republication not permitted without written consent of the publisher

1. INTRODUCTION

Hydrothermal vents are underwater dynamic physical and chemical ecosystems driven by the heating up of hydrothermal vent fluids (>400°C) and discharging at the seafloor under high-temperature and high-pressure conditions. This leads to enrichment in dissolved components including metals and acidic gases, especially carbon dioxide (Kelley et al. 2002). In addition to deep-sea hydrothermal vent biological studies, there has recently been a surge in research on shallow-water vents, such as in Italy (Hall-Spencer et al. 2008, Lucey et al. 2016, Saidi et al. 2023, D'Alessandro et al. 2024) and Japan (Agostini et al. 2015, 2018), to use natural high carbon dioxide systems to simulate conditions of future ocean acidification. The activity of animals inhabiting hydrothermal vents can be coupled with the dynamic physical environments of the vents. Understanding the activity patterns of vent animals in relation to the physical environment can allow us to understand how vent animals adapt and survive in these harsh environments. However, research focusing on this aspect is rare due to

*Corresponding author: tychan@mail.ntou.edu.tw

© Inter-Research 2024 · www.int-res.com

technical limitations (including tackling strong currents, high pressure, and long-term battery supplies) in establishing time-lapse or video cameras for long-term observations in the harsh vent environment.

Tunnicliffe et al. (1990) were the first to install underwater time-lapse cameras in the deep-sea hydrothermal vents at the Juan de Fuca Ridge in the northeast Pacific to observe the behavior of ventimentiferan worms for up to 32 d. Extension and retraction movements of the ventimentiferan worms revealed semidiurnal and diurnal activity but were not significantly related to surrounding currents or suspended particulates. Bates et al. (2010) conducted laboratory aquarium experiments and found that deep-sea scale worms, limpets, and snails preferred to stay in locations with cooler temperatures under a continuum of temperature ranges in the aquarium, and this correlates with *in situ* observations that vent organisms are gathered at the locations with cooler waters.

Compared to ventimentiferan worms and mollusks, crustaceans including crabs, galatheids, and shrimps are highly mobile fauna and are present in both deep-sea and shallow-water hydrothermal vents. However, at present, no study has investigated the activity patterns of vent crustaceans and their relations to dynamic vent environments. The vent crab *Xenograpsus testudinatus* (Xenograpsidae) is common in shallow- and deep-water hydrothermal vents from 10 to >300 m in depth in the NW Pacific region, including the Kueishan Island vents in Taiwan (Fig. 1; Jeng et al. 2004, Wang et al. 2014, Yang et al. 2022). Two types of vents, characterized by their temperature ranges, are found in the Kueishan Island vent region. Yellow vents are hot and acidic (78–116°C and pH 1.52–6.32 at vent openings), whereas white vents are relatively cooler but have similar acidity (30–65°C and pH 1.84–6.96). The water temperature of vent regions is strongly affected by tidal currents, whereby high tides exert greater pressure on the vent fluids and thus create a hotter environment (Chen et al. 2005). The inorganic and organic compounds released from these vents create a strong biochemical gradient in the surrounding environment (e.g. decreasing water temperature and increasing pH and dissolved oxygen), consequently leading to a change in species richness and biodiversity from vent mouths to peripheral regions (Chan et al. 2016). The density of vent crabs is highest in the vent region and lower in the peripheral region (100 m away from vents), and crabs were absent from regions farther from the vent periphery towards non-vent regions (Chan et al. 2016). *X. testudinatus* has no obligate nutritional dependence on chemoautotrophic sources (T. Wang et al. 2014, 2022, Chang et al. 2018, Wu et al. 2021, Y. Wang et al. 2023), and *X. testudinatus* in Kueishan Island mainly feeds on marine snow generated from the dead zooplankton killed by vent plumes (Jeng et al. 2004, Hu et al. 2012), algae, particulate organic matter, and also large-sized carcasses in the vent (Wang et al. 2022).

Intertidal decapod crustaceans, including crabs, can exhibit rhythmic behavioral patterns to synchronize their activity with external environmental variables, including tidal cycles (e.g. Bradshaw & Scoffin

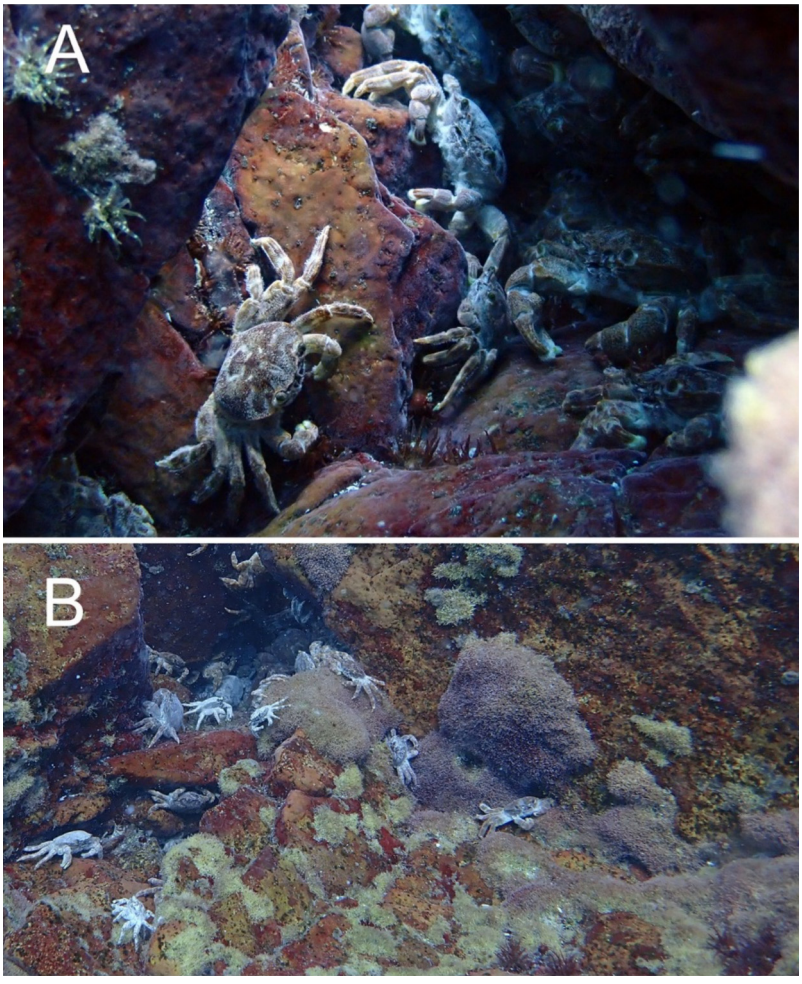

Fig. 1. (A) Hydrothermal vent crabs *Xenograpsus testudinatus* are common in shallow-water hydrothermal vents in the NW Pacific region. (B) *X. testudinatus* often appear as large, aggregated populations in vent regions

1999, Moriyama et al. 2017, Pombo et al. 2018), day–night cycles (e.g. Bradshaw & Scoffin 1999, Nordhaus et al. 2009, Mat et al. 2017, Moriyama et al. 2017, Pombo et al. 2018), monthly spring–neap cycles (Zeng et al. 1999, Al-Wazzan et al. 2018), and annual seasonal changes (Styrishave et al. 1999, Luppi et al. 2013). It is possible that vent crabs inhabiting shallow-water hydrothermal vents can have their activity affected by such a dynamic physical environment. Jeng et al. (2004) conducted daytime SCUBA diving to observe *X. testudinatus* and proposed a hypothesis that these vent crabs may emerge from crevices in large swarms to feed during slack water at the highest and lowest tides. During these slack tide periods, dead plankton can directly sink down to the bottom when there are only weak or no currents. However, vent crabs may also respond to diurnal variations in water temperature generated from the interactions of the vent plumes and tides. To test these hypotheses and examine temporal variation in the activity of shallow-water vent crabs, it is essential to establish an *in situ* underwater monitoring system with adequate battery life for multi-day recording and infrared lighting at night. The system should also be robust enough to withstand the strong current and acidic vent environment. Deep-sea time-lapse cameras for observation of animal diurnal activities are not suitable for use in shallow water vents due to their large size, and they can be easily dislodged by strong tidal currents.

In the present study, we developed a novel underwater time-lapse camera system (with infrared lights and recording sensors) and a stainless supporting frame that allows the camera system to be established in shallow-water vents to take 3–4 d of time-lapse photographs for each consecutive sampling period. Based on the use of this camera system to record the activity of vent crabs, we tested the hypotheses that vent crabs have rhythmic activity patterns and that crab density is maximum during the slack water periods at the highest and lowest tides as proposed by Jeng et al. (2004). We also tested the hypothesis that the crab activity pattern is correlated to tide levels, water temperature, pH, and light intensity.

2. MATERIALS AND METHODS

2.1. Study sites and data sampling

The shallow-water hydrothermal vent study site (121.962° E, 24.834° W) is located approximately 100 m from the shoreline of Kueishan Island at depths of 15–18 m (Fig. 2A–C; also see Chan et al. 2016).

To compare the activity of vent crabs in the vent and peripheral regions, 3 underwater time-lapse cameras (see Section 2.2) were installed in the area with the strongest yellow vent plumes and high populations of *Xenograpsus testudinatus*, and 2 other cameras were established in peripheral sites about 30 m away from vents but still with the presence of *X. testudinatus* (Fig. 2D). All cameras faced towards large areas of relatively flat vertical or inclined rocks without any crevices so that the crabs walking on the rock surfaces could be easily filmed.

Time-lapse photograph recording started at the same time in a total of 5 periods between 10 August and 25 November 2018 with a duration of 2–3 d at each sampling time, covering variations in tide patterns, moon phases, and seasons. For the 3 vent cameras, the cameras were set in 3 additional periods from 23 December 2018 to 17 August 2019, with a duration of 1–3 d in each recording period. All cameras were installed at a distance of 65 cm from the filming locations to obtain images of an area of 89 × 50 cm.

HOBO Pendant Temperature/Light 64K Data Loggers were attached to the sides of all the underwater cameras from the beginning of the study. HOBO Bluetooth Low Energy pH and Temperature Data Loggers were also attached to the cameras at the vent area from the 2nd to 6th trials between 2 September and 25 December 2018. In the peripheral area, a HOBO Bluetooth Low Energy pH and Temperature Data Logger was attached to 1 of the cameras between 13 and 25 November 2018. Cameras were set at a time lapse of 5 s, with infrared mode (i.e. taking black and white photographs based on infrared light source) from 18:35 to 05:15 h on each day of sampling.

2.2. Underwater monitoring system

The monitoring system included an underwater camera housing with a battery (2XD type)-powered time-lapse surveillance camera (Brinno MAC200 DN), securely fixed on a stainless frame for long-term monitoring of crab activities (Fig. 3). The time-lapse camera used in the present study can also capture infrared photographs at night. To take time-lapse photographs at night, a custom-made stainless steel underwater housing for infrared light and a separate battery supply (18A, 12V) capable of lasting for at least 36 h of usage was used as the light source at night. Infrared lighting was employed at night to avoid any artificial visible light that may disturb the

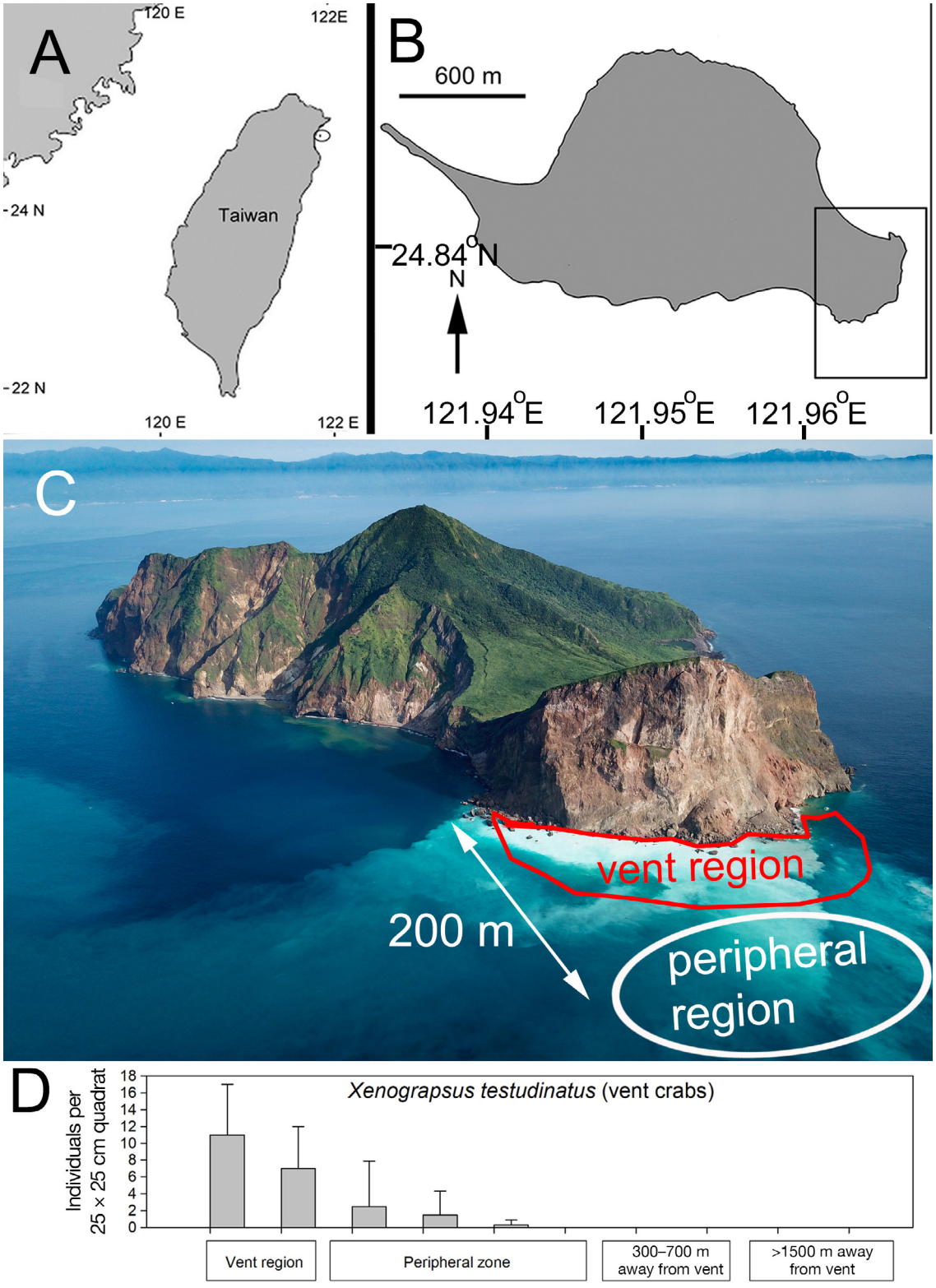

Fig. 2. (A) Taiwan, showing the location of Kueishan Island (circled). (B) Kueishan Island. Rectangle denotes the vent region shown in panel C. (C) Aerial photograph of Kueishan Island, showing the location of the vent region and peripheral region. (Photo courtesy of Huai Su) (D) Variation in abundance of *Xenograpsus testudinatus* from the vent to the peripheral region; data extracted from Chan et al. (2016)

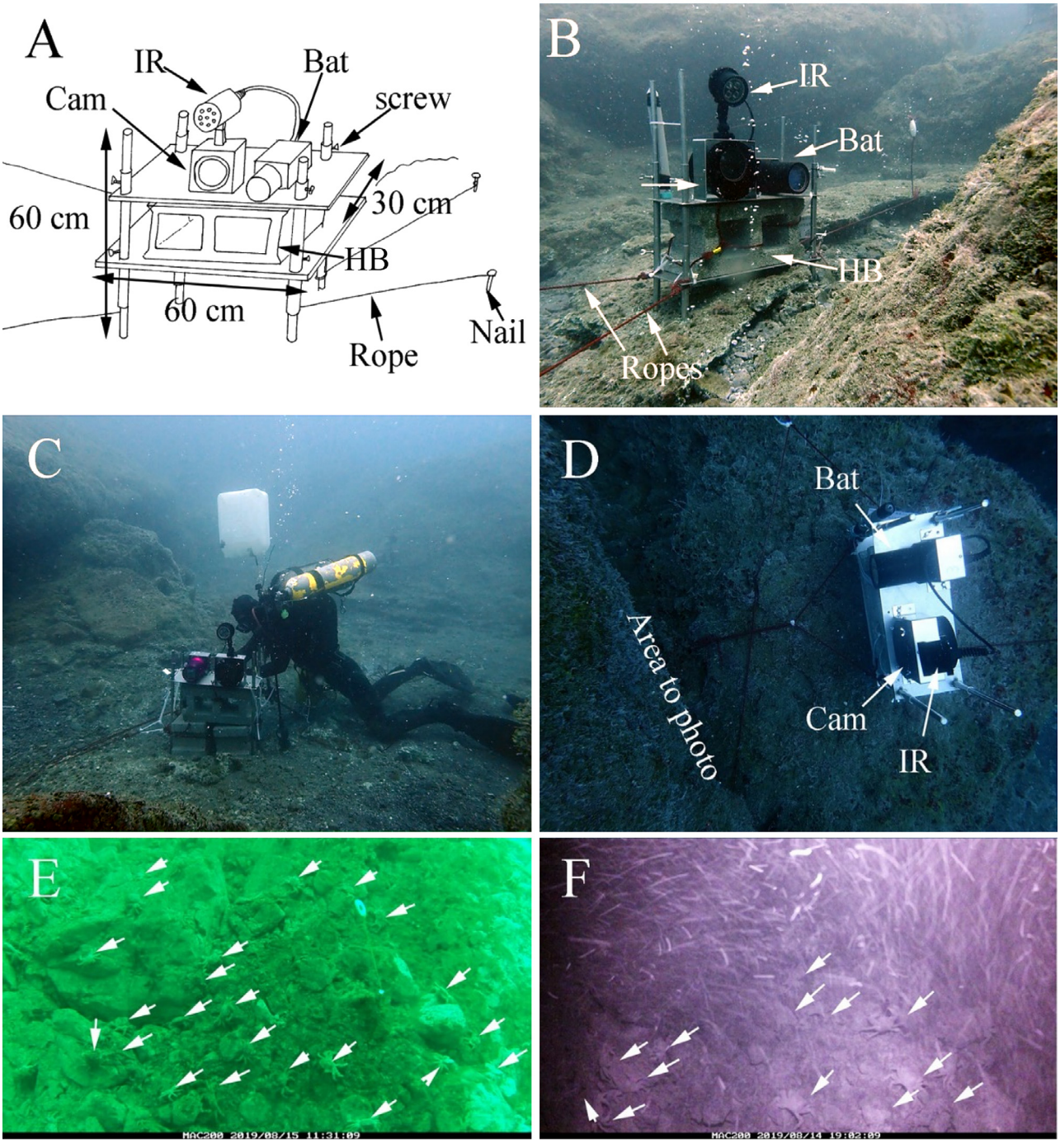

Fig. 3. (A) Underwater time-lapse camera system, including the underwater housing with the time lapse camera (Cam), installed with an infrared light (IR) which has a sensor for turning on during low light intensity. The infrared light is supported by a long-life rechargeable battery (Bat) inside an underwater housing. The whole monitoring system was flexibly mounted on a movable stand, with 4 adjustable legs to fit the irregular substratum. The stand has a hollow brick (HB) to act as a weight for stabilizing underwater. The stand is fixed on the substratum using 4 stainless steel nails and ropes. (B) The camera system with the stand established in the vent region. (C) Installing the system on site using SCUBA diving with 2 air tanks to accommodate the long work time underwater. (D) The camera system viewed from the top. (E) Photograph taken by the time-lapse camera during the daytime, showing swarming crabs (indicated by white arrows). (F) Photograph taken by the time-lapse camera at night using infrared lighting. White arrows indicate the crabs identified in the photograph

natural activity of vent crabs (Fig. 3). The underwater infrared lights had built-in light sensors and automatically switched on during low light intensity.

Due to the heavy deposits of sulfur crystals and other suspended matter from hydrothermal vents, the camera housing sometimes had the porthole partly or completely blocked within less than 1 d and hence did not yield usable footage for analysis. In some cases, suspended matter was too dense, and strong bubbling from vents prevented the infrared light from reaching the target areas, resulting in some of the photographs taken at night not being usable. The highly corrosive water and heavy sulfur deposits in vents also damaged the sensors of all 4 pH meters used in this study at the end of 2018. We successfully recorded time segments of 354 and 162 h of recording in vent and peripheral regions, respectively.

2.3. Data and statistical analysis

Only footage consisting of acceptable quality images from more than 24 consecutive hours was analyzed. Data analysis involved counting the number of crabs and fishes (predators) within an area of 50 × 50 cm in each calibrated photograph. The occurrence of fishes (indication of predator abundance) in the vent and peripheral regions was recorded to examine whether there were variations in predator frequencies between these 2 regions. A crab or fish located between the inside and outside of the quadrat area (partial view of a body) was also considered as 1 crab or fish. Mean crab abundance per hour was scored from 12 photographs (at 5 min intervals) from a single hour. Photographs with low visibility due to blocking by vent bubbles, sulfur deposits, or plankton were discarded and replaced by a randomly chosen photograph with acceptable quality based on the following criteria and priority: (1) at least 1 min later than the original photograph, (2) if no subsequent photograph could be used, a previous photograph from within the same hour was randomly selected. Fishes seen in the photographs were counted and identified to the family level. Tidal data were obtained by referring to the tidal records at Wushih harbor (marine observatory station nearest to Kueishan Island) of the Central Weather Bureau, Taiwan.

Time series analysis (Sigma XL) was conducted to examine the temporal variation in crab density (averaged from 3 cameras at hourly intervals in the vent region and from 2 cameras at each hour interval in the peripheral region), tides, water temperature, and pH from the combined multiple segments of time-lapse data, covering 354 h in the vent region and 162 h in the peripheral region. Autocorrelation and spectral density plots were created for crab density, tides, pH, water temperature, and light intensity to examine any rhythmic patterns. Cross correlation analysis was conducted to examine any relationship between crab density and tides, water temperature, pH, and light intensity. Pearson correlation and regression coefficients were calculated among various combinations of crab density, water temperature, tide levels, pH, and light intensity. Stepwise multiple regression (backward) was conducted to identify the significant environmental predictors of crab density including water temperature, tide levels, pH, and light intensity in the vent and rim region separately, using the software SigmaPlot 11 (Grafiti). Crab density was cubic root transformed to pass the constant variance test (SigmaPlot 11) in both vent ($p = 0.064$) and rim regions ($p = 0.445$).

To test the hypothesis that crab density is highest during the slack tide periods (i.e. at the highest and lowest tides), crab density in the vent region (where crab densities were greater) at each of the highest tide, lowest tide, and rising and lowering tide periods (midpoint between lowest and highest tide) during the daytime and at night were recorded, where the hours from 07:00 to 18:59 h were considered daytime, and from 19:00 to 06:59 h on the following day were regarded as night. Spring tides were defined as the maximum amplitude of tide >2 m, and the amplitude of neap tides was <1.5 m. Variation in crab density among different tide periods (factor: tide) in the daytime and at night (factor: day–night) was compared using 2-way ANOVA (factors: day–night and tides) using the software SigmaPlot 11. Crab density was square-root transformed and passed the constant variance test ($p = 0.799$) and the Shapiro-Wilk normality test ($p = 0.289$).

3. RESULTS

3.1. Vent region

Average crab abundance varied from 0 to 25 individuals per 50 × 50 cm quadrat for the 354 h recorded. Crab density was variable within a day and among days (Fig. 4). Within a day, there were 3–5 peaks and troughs of crab density (Fig. 4). The average density of crabs was lowest during 2–5 September 2018 (Fig. 4). Water temperatures recorded in the vent region had 3–4 daily peaks and troughs, with the maximum often reaching about 30°C. Water temperatures dropped to

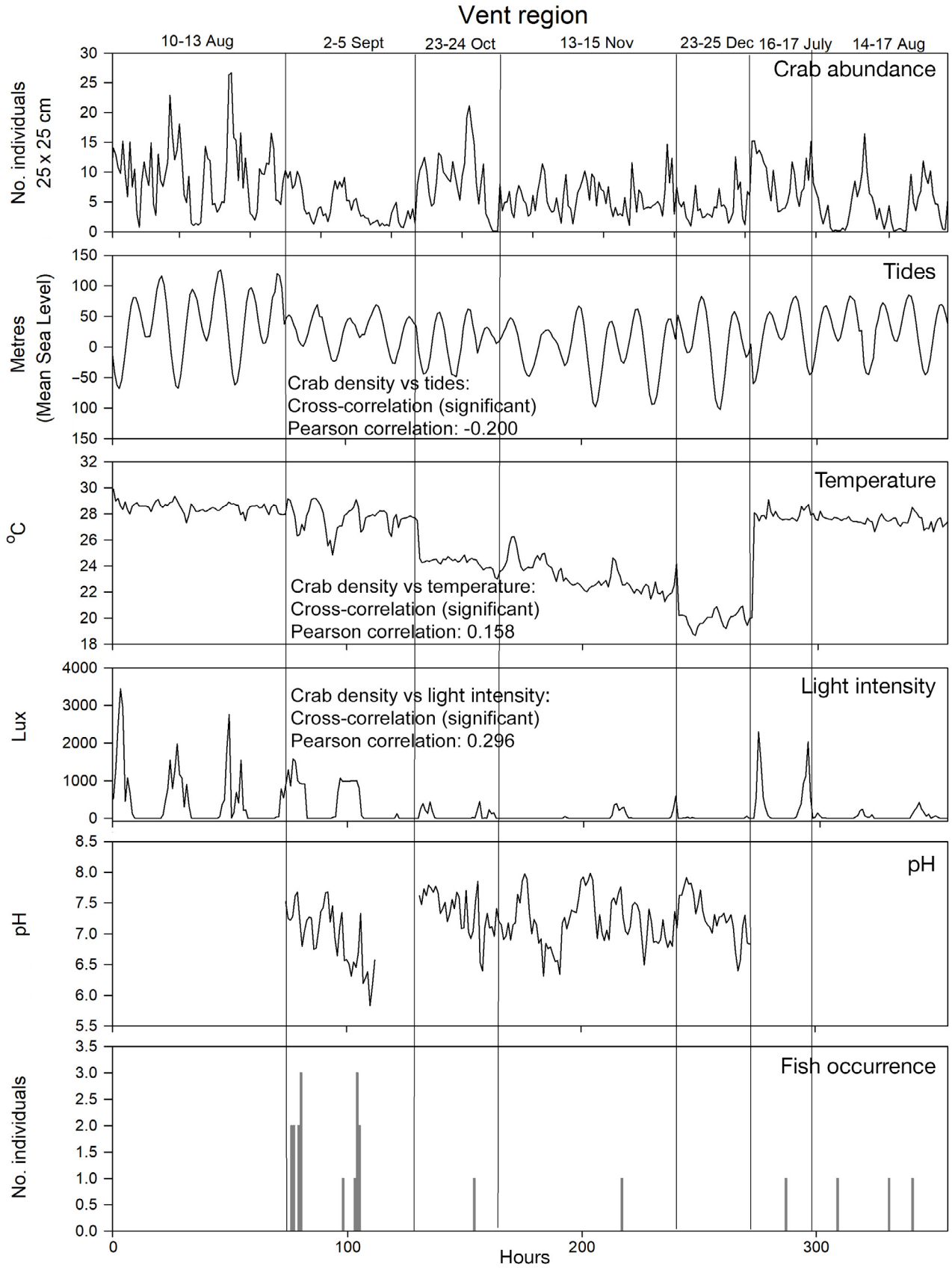

Fig. 4. Time series data of *Xenograpsus testudinatus* abundance, tide levels, water temperature, light intensity, pH, and fish occurrence from 354 h data points in the vent region from 10 August 2018 to 17 August 2019

19–26°C during winter months (October–December) but still had 2–3 peaks and troughs on most days (Fig. 4). pH was recorded in September to December samplings. pH fluctuated between 5.9 and 7.9 during the sampling period, with 3–5 peaks and troughs at daily intervals (Fig. 4). Light intensity appeared to follow a diurnal cycle, with greater light intensity during the daytime (Fig. 4). However, on most days, even during the daytime, only very weak light intensity was recorded, probably because the top layer of the seawater was masked by the white and yellowish vent effluents. Fishes (family Chaetodontidae and Gobiidae) were seen occasionally. A total of 28 fish were recorded in 354 h (average 0.07 fish h^{-1}, Fig. 4).

To examine the periodicity of the activity patterns of crabs and the environmental parameters, autocorrelation analysis showed that temporal variation in crab density had a significant correlation with time lags up to 4 h. Autocorrelation analysis of tide levels indicated significant correlations with time lags from 0 to 6 h and then from 11 to 13 h (Fig. S1 in the Supplement at www.int-res.com/articles/suppl/m744p069_supp.pdf). Autocorrelation analysis on pH revealed a significant correlation up to 5 h (Fig. S1). Autocorrelation analysis on water temperature revealed a significant correlation up to 23 h (Fig. S1). Spectral density plots of tide levels revealed a significant peak at 13 h (Fig. S2). However, no significant peaks were identified in the spectral density plots of crab density, water temperature, and pH, indicating that these temporal variations are not rhythmic.

Cross correlation analysis on crab density to tides revealed a negative significant correlation ranging from +1 to −2 h time lags (maximum coherence was 0.2 at time lag = 0; Table 1, Fig. S3). Pearson correlation between crab density and tides revealed a significant negative correlation (correlation coefficient −0.204, p = 0.0001; Fig. S4). Cross correlation on crab density to water temperature revealed a positive correlation from 0 to −9 h time lags (coherence was 0.1–0.15 from 0 to 1 h time lag) (Table 1, Fig. S3). Pearson correlation between crab density and water temperature revealed a significant positive correlation (0.158, p = 0.0028; Fig. S4). Cross correlation analysis on crab density to light intensity revealed a significant correlation in the range of −5 to + 5 h time lags (maximum coherence 0.39 at +2 time lag). Pearson correlation had a significant positive correlation on crab density and light intensity (0.296, p < 0.0001; Fig. S4). Cross correlation between crab density and pH did not reveal a significant relationship at −4 to + 4 time lags, with only the time lag at +9 having a significant relationship, with coherence 0.2 (Table 1, Fig. S3).

Table 1. Cross-correlation analysis on the significant coherence (p < 0.05) from a 354 h time series of selected variables in the vent region from time lags −3 to + 3 h (for the total analysis up to 50 h, see Fig. S1 in the Supplement). High positive coherence value indicates a high correlation between the 2 variables at a specific time lag

Variable A	Variable B	Time lag (h)	Coherence (p < 0.05)
Crab density	Water temperature	−2	−0.14
		−1	−0.19
		0	−0.15
		1	−0.20
Crab density	Tide level	−3	0.14
		−2	0.15
		−1	0.16
		0	0.15
		1	0.10
Crab density	Light intensity	−3	0.20
		−2	0.29
		−1	0.30
		0	0.29
		1	0.38
		2	0.39
		3	0.30
Water temperature	Tide	−3	0.29
		−2	0.30
		−1	0.30
		0	0.31
		1	0.31
		2	0.30
		3	0.28

Table 2. Cross-correlation analysis on the significant coherence (p < 0.05) from a 162 h time series of crab density and tide level in the peripheral region from time lags −3 to + 3 hours (for the total analysis up to 50 h, see Fig. S7). High coherence indicates high correlation between the 2 variables at a specific time lag

Variable A	Variable B	Time lag (h)	Coherence (p < 0.05)
Crab density	Tide level	−3	0.37
		−2	0.40
		−1	0.39
		0	0.29
		1	0.15
Water temperature	Tide level	−3	0.37
		−2	0.41
		−1	0.45
		0	0.47
		1	0.45
		2	0.42
		3	0.37

Pearson correlation analysis on crab density and pH did not reveal a significant correlation (p = 0.140).

There was a positive cross-correlation between tide and water temperature at a wide range of time lags, with coherences generally reaching 0.3 (Table 1).

There was no significant cross correlation between tide level and pH. Among the environmental factors, the Pearson correlation revealed a positive relationship between water temperature and tide (0.305, $p < 0.0001$) and between water temperature and light intensity (0.308, $p < 0.0001$). However, Pearson's correlation indicated that tide level was significantly negatively correlated with pH (−0.163, $p < 0.007$).

Light intensity was considered as a significant predictor for crab density in backward stepwise multiple regression ($R = 0.186$, $R^2 = 0.034$). The model was significant ($F_{1,179} = 6.395$, $p < 0.012$). The predicted crab density = (0.000213) × light intensity + 1.701.

3.2. Peripheral region

Time-lapse photography of the peripheral region yielded 162 h of recordings. Crab density fluctuated between 0 and 5 individuals per 50 × 50 cm quadrat throughout the recording periods. There were about 2–4 peaks and troughs of crab densities within a day (Fig. 5). The daily density fluctuations of crabs were similar throughout the recording period from September to November. Water temperature exhibited 3–4 peaks and troughs of fluctuation per day, and the temperature ranged from 24 to 28°C (Fig. 5) in September and from 23 to 25°C in November. There were 2–3 daily peaks and troughs in temperature (Fig. 5). Recorded light intensity was low even during the daytime, probably due to the masking effect of the vent effluents at the surface layer (Fig. 5). pH varied from 6.6 to 8.2, with 2–3 maxima and minima in 1 d (Fig. 5). Fishes (family Chaetodontidae and Gobiidae) were seen in some periods, with a maximum of 24 fishes recorded in 1 h. A total of 98 fishes were recorded in 162 h (average 0.6 fish h^{-1}, Fig. 5).

Autocorrelation analysis on the time series data of crab density indicated a significant correlation of time lags of 1–2 h. Autocorrelation analysis of tide levels indicated significant correlations of time lags up to 3 h and then again at 7 h (Fig. S5). Autocorrelation analysis on pH revealed a significant correlation up to 2 h. Autocorrelation analysis on water temperature revealed a significant correlation up to 12 h. Spectral density plots on tides only revealed a significant repeatable pattern at 13 h (Fig. S6), whereas spectral density plots of crab density, water temperature, and pH did not have significant peaks, suggesting that these variations are not rhythmic.

Cross-correlation analysis on crab density and tides revealed a positive significant correlation from +1 to −4 h time lags (Table 2, Fig. S7), with the highest coherence of 0.4 at a time lag of −2 h. Pearson correlation between crab density and tides revealed a significant positive correlation (correlation coefficient 0.300, $p < 0.05$; Fig. S8). Cross-correlation on crab density and water temperature, light intensity, and pH did not reveal any significant correlations. Pearson correlation between crab density and water temperature and light did not reveal any significant correlation ($p > 0.05$). Pearson correlation revealed a significant negative correlation between crab density and pH (−0.280, $p = 0.0003$; Fig. S8).

There was a positive cross-correlation between tide and water temperature at a wide range of time lags (Fig. S7E). Pearson correlation revealed a positive relationship between water temperature and tide (0.448, $p < 0.0001$) (Table 2).

Tide levels were considered significant environmental variables in step-wise multiple regression analysis for predicting crab density. The model was significant ($F_{1,95} = 13.664$, $p < 0.001$; $R = 0.355$, $R^2 = 0.126$). Predicted crab density = (0.0032) × tide + 1.032.

3.3. Variations in crab density among tide periods

There was no significant variation in crab densities between day and night, among periods of highest and lowest spring and neap tides, or between the rising and falling of spring and neap tides at day and night (2-way ANOVA; Table 3, Fig. 6). There were large variations in crab densities within each of these tide periods, resulting in the variation in crab densities among the tide periods in daytime and night not being significant (Fig. 6, Table 3).

4. DISCUSSION

This is the first known study using continuous, multiple days with 24 h *in situ* underwater observations of the activity pattern of the subtidal shallow-water hydrothermal vent crab *Xenograpsus testudinatus*. Our results showed that the activity of *X. testudinatus* did not have a rhythmic or repeatable pattern. However, the activity of the crabs in the vent region was affected by the interaction of water temperature, tide levels, and light intensity (Fig. 4, Table 1). Multiple regression modeling showed that light intensity had the greatest influence on crab density among other significant factors in the correlation analysis. Crabs in the peripheral region had a lower density compared to around the vents, and multiple regression suggested the activity was mainly affected by tides (Fig. 5, Table 2).

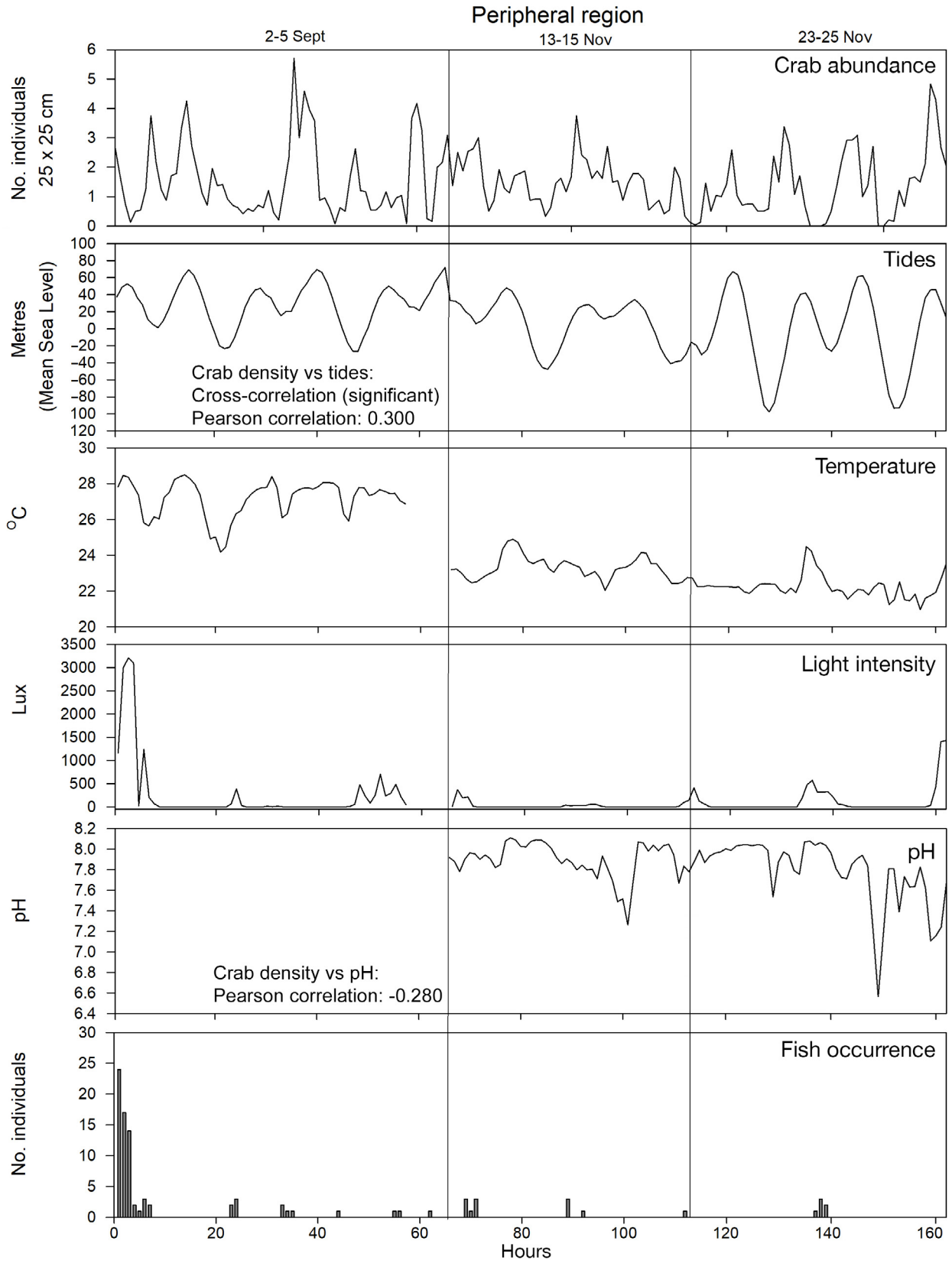

Fig. 5. Time series data of *Xenograpsus testudinatus* abundance, tide levels, water temperature, light intensity, pH, and fish occurrence from 162 h data points in the peripheral region from 2 September to 25 November 2018

Table 3. Two-way ANOVA analyzing the variation in density of *Xenograpsus testudinatus* between day and night (factor day—night) and among 8 tidal periods. Density of *X. testudinatus* was square root transformed to meet assumptions of normality (Shapiro-Wilk test, p = 0.289) and homogeneity of variances (constant variance test, p = 0.799)

Factor	df	MS	*F*	p
Day—night	1	1.779	2.276	0.135
Tides	7	0.413	0.528	0.811
Day—night × Tides	7	0.523	0.669	0.698
Residual	100	0.782		

Many intertidal invertebrates including limpets and fiddler crabs have circatidal or circalunar behavioral rhythms in feeding, reproduction, or mating activity in relation to the tidal cycle (de la Iglesia & Johnson 2013). However, *X. testudinatus* did not show circatidal activity; rather, activity appeared to be plastic and could be affected by the environment. The density of *X. testudinatus* was negatively correlated with tide levels in the vent region but vice versa in the peripheral region. Cross-correlation analysis indicated that crabs can respond within 1 to 2 h before and after the tide level changes. Higher abundance of crabs in the vent region at lower tide levels may be due to water becoming more acidic (note that pH was negatively correlated with tide level in the vent region), as *X. testudinatus* can well adapt to a lower pH environment (Allen et al. 2020). The pH in the vent region was significantly negatively correlated with tide level. In the peripheral region further away from the acidic sources at vent plumes, there was no correlation between pH and tide levels. More crabs came out during higher tide levels, likely related to foraging, as subtidal crabs are generally more active during higher tide levels (Hadlock 1980, Reid & Naylor 1989, Chatterton & Williams 1994). The present results do not support the hypothesis that *X. testudinatus* come out in large swarms to feed during slack water in periods of the highest and lowest tides (Jeng et al. 2004). There were large variations in crab density among different tide periods, and we found no significant difference in crab density among tide periods (Fig. 6, Table 3). The observations by Jeng et al. (2004) were only made during the daytime, but we found that *X. testudinatus* at vents do not often form distinct large swarms during the highest and lowest tides in day- and nighttime (Fig. 6, Table 3).

The density of *X. testudinatus* in vent regions appears to be affected by light intensity and was significantly higher during periods with high light intensity during the daytime (sunny weather or thinner layer of the white coloured vent water on the surface). The long hours of solar illumination during the daytime may explain why the response of crab density to light intensity can have time lags up to several hours as reflected in the cross-correlation analysis. However, *X. testudinatus* was not completely inactive during the night. In the peripheral area, there was no significant correlation between the density of crabs and light intensity. The limited studies on the diurnal activities of subtidal crabs generally showed that crabs are mainly nocturnal to avoid predation during the daytime (Chatterton & Williams 1994, Skajaa et al. 1998, Takahashi & Kawaguchi 2001, Shmuel et al. 2022). The extreme conditions of hydrothermal vent regions render a predator-free environment (Voight 2000). The significantly higher density of *X. testudinatus* during the daytime compared to night is likely due to the lower abundance of predators (average fish abun-

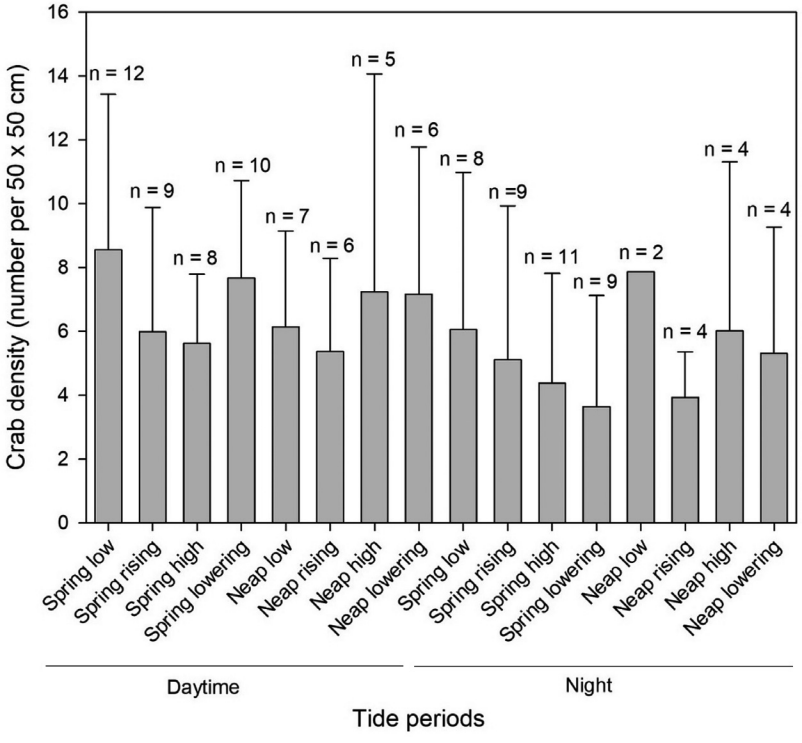

Fig. 6. Variation in mean (+1 SD) crab density during different tide periods in daytime and at night. Two-way ANOVA revealed that variation in crab density among tide periods and between daytime and nighttime was not significant. Significance level is at $\alpha = 0.05$

dance 0.07 h^{-1}) when compared to the peripheral region (average fish abundance 0.6 h^{-1}). The presence of predators can affect the activity of crabs. The unusual diurnal activity in commercial subtidal crabs of the genera *Cancer* and *Carcinus* in the Gulf of Maine was suggested to be related to behavioral changes following the removal of their main predators, i.e. cod and haddock, as a result of overfishing (Novak 2004).

The vent region has higher occurrence frequencies of high temperature (>28°C) and low pH (<6.5) when compared to the peripheral region. There was a significant but weak positive correlation between crab activities and water temperature in the vent region (Table 1). As *X. testudinatus* is a dominant animal in the hydrothermal vent, its preference for higher temperatures is not unexpected. Nevertheless, such a correlation was less clear in the peripheral region (Table 2), probably because of the lower fluctuation range of temperature variation. In the peripheral region, crab abundance was negatively correlated with pH, such that the more acidic the water was, the more crabs emerged. There are likely fewer predators in the acidic environment. This concurs with the ability of vent crabs to adapt to a more acidic environment (Allen et al. 2020). Recent physiological studies have also proved that *X. testudinatus* adapts to environments rich in hydrogen sulfide mainly by means of detoxification in gills and endo-symbiotic bacteria in gills (Chen et al. 2023, Chou et al. 2023). In the vent region, there was generally no correlation between pH and crab abundance. The non-significant correlation of pH with crab density in the vent areas is likely because the pH environment in the vent regions is more extreme, and very few predators can enter this region. *X. testudinatus* is nearly absent from non-vent areas off Kueishan Island, which has pH values of around 8.1 (Chan et al. 2016), similar to other oceans (Garcia-Soto et al. 2021). The non-vent region has numerous predatory fishes, and this explains the near absence of *X. testudinatus* in these areas (Chan et al. 2016).

Time-lapse photography is an important technique to document time series of animal behavior. The shallow-water hydrothermal vent environment presents many challenges when establishing time-lapse photography studies. Although we successfully used a newly designed long-life battery-powered infrared underwater camera, which can work for 3–4 d, to continuously monitor subtidal crabs, the strong currents and acidic environmental conditions of hydrothermal vents did not allow us to obtain more than one consecutive day of images due to dislocation of the illumination angle of the infrared light, and these data were not used for analysis. Rapid deposition of sulfur and organic deposits can mask the glass on the camera housing and result in failure to obtain successful longer continuous monitoring. Biofouling issues are also encountered in deep-sea hydrothermal vent observations, and microchlorination has been suggested to lessen this problem (Auffret et al. 2009). However, the shallow-water vents off Kueishan Island often have strong currents (Chen et al. 2005) that can stir up the rich sulfur and suspended matter. Innovative techniques will need to be developed to overcome the heavy fouling problems to gain longer consecutive daily observations on the animals inhabiting these vents.

In conclusion, time-series analysis on the activity of the hydrothermal vent crab *X. testudinatus* revealed that this crab forages at all times, but it is more active during the day at the vent region. Our results do not support the hypothesis that *X. testudinatus* forms large swarms during slack tides. Instead, *X. testudinatus* activity around vents is significantly correlated with the interactions of water temperature, day–night cycle, and tide level, with more crabs emerging at higher temperatures but lower tide levels during daytime. In the peripheral region, crab activity was affected by the interaction of tides and pH. *X. testudinatus* is more active during high tides for feeding, and also during periods with lower pH, which may cause a reduction in the number of predators entering this region.

Acknowledgements. This work was supported by grants from the National Science and Technology Council, Taiwan, ROC, and the Center of Excellence for the Oceans (National Taiwan Ocean University), which is financially supported by The Featured Areas Research Center Program within the framework of the Higher Education Sprout Project by the Ministry of Education (MOE) in Taiwan, ROC. B.K.K.C. was supported by research funding from the Biodiversity Research Center, Academia Sinica, Taiwan. Thanks to Huai Su for providing the copyright for the use of the image in Fig. 2C.

LITERATURE CITED

Agostini S, Wada S, Kon K, Omori A and others (2015) Geochemistry of two shallow CO_2 seeps in Shikine Island (Japan) and their potential for ocean acidification research. Reg Stud Mar Sci 2:45–53

Agostini S, Harvey BP, Wada S, Kon K, Milazzo M, Inaba K, Hall-Spencer JM (2018) Ocean acidification drives community shifts towards simplified non-calcified habitats in a subtropical–temperate transition zone. Sci Rep 8:11354

Al-Wazzan Z, Le Vay L, Behbehani M, Giménez L (2018) Hatching rhythm and larval release in *Leptodius exaratus*

(H. Milne Edwards, 1834) (Decapoda: Brachyura: Xanthidae) from rocky shores in Kuwait. J Crustac Biol 38: 804–811

Allen GJP, Kuan PL, Tseng YC, Hwang PP, Quijada-Rodriguez AR, Weihrauch D (2020) Specialized adaptations allow vent-endemic crabs (*Xenograpsus testudinatus*) to thrive under extreme environmental hypercapnia. Sci Rep 10:11720

Auffret Y, Coail JY, Delauney L, Legrand J and others (2009) Tempo-Mini: a custom-designed instrument for real-time monitoring of hydrothermal vent ecosystems. Instrum Viewpoint 8:17

Bates AE, Lee RW, Tunnicliffe V, Lamare MD (2010) Deep-sea hydrothermal vent animals seek cool fluids in a highly variable thermal environment. Nat Commun 1:14

Bradshaw C, Scoffin TP (1999) Factors limiting distribution and activity patterns of the soldier crab *Dotilla mycti-roides* in Phuket, South Thailand. Mar Biol 135:83–87

Chan BKK, Wang TW, Chen PC, Lin CW, Chan TY, Tsang LM (2016) Community structure of macrobiota and environmental parameters in shallow water hydrothermal vents off Kueishan Island, Taiwan. PLOS ONE 11:e0148675

Chang NN, Lin LH, Tu TH, Jeng MS, Chikaraishi Y, Wang PL (2018) Trophic structure and energy flow in a shallow-water hydrothermal vent: insights from a stable isotope approach. PLOS ONE 13:e0204753

Chatterton TD, Williams BG (1994) Activity patterns of the New Zealand cancrid crab *Cancer novaezelandiae* (Jacquinot) in the field and laboratory. J Exp Mar Biol Ecol 178:261–274

Chen CTA, Zeng Z, Kuo FW, Yang TF, Wang BJ, Tu YY (2005) Tide-influenced acidic hydrothermal system offshore NE Taiwan. Chem Geol 224:69–81

Chen C, Wu GC, Chung YT, Li HW and others (2023) Duplicated paralog of sulfide: quinone oxidoreductase contributes to the adaptation to hydrogen sulfide-rich environment in the hydrothermal vent crab, *Xenograpsus testudinatus.* Sci Total Environ 890:164257

Chou PH, Hu MY, Guh YJ, Wu GC and others (2023) Cellular mechanisms underlying extraordinary sulfide tolerance in a crustacean holobiont from hydrothermal vents. Proc R Soc B 290:20221973

D'Alessandro M, Gambi MC, Bazzarro M, Caruso C and others (2024) Characterization of an undocumented CO_2 hydrothermal vent system in the Mediterranean Sea: implications for ocean acidification forecasting. PLOS ONE 19:e0292593

de la Iglesia HO, Johnson CH (2013) Biological clocks: riding the tides. Curr Biol 23:R921–R923

Garcia-Soto C, Cheng L, Caesar L, Schmidtko S and others (2021) An overview of ocean climate change indicators: sea surface temperature, ocean heat content, ocean pH, dissolved oxygen concentration, arctic sea ice extent, thickness and volume, sea level and strength of the AMOC (Atlantic Meridional Overturning Circulation). Front Mar Sci 8:642372

Hadlock RP (1980) Alarm response of the inter-tidal snail *Littorina littorea* (L.) to predation by the crab *Carcinus maenas* (L.). Biol Bull (Woods Hole) 159:269–279

Hall-Spencer JM, Rodolfo-Metalpa R, Martin S, Ransome E and others (2008) Volcanic carbon dioxide vents show ecosystem effects of ocean acidification. Nature 454: 96–99

Hu MYA, Hagen W, Jeng MS, Saborowski R (2012) Metabolic energy demand and food utilization of the hydrothermal vent crab *Xenograpsus testudinatus* (Crustacea: Brachyura). Aquat Biol 15:11–25

Jeng MS, Ng NK, Ng PKL (2004) Hydrothermal vent crabs feast on sea 'snow'. Nature 432:969

Kelley DS, Baross JA, Delaney JR (2002) Volcanoes, fluids, and life at mid-ocean ridge spreading centers. Annu Rev Earth Planet Sci 30:385–491

Lucey NM, Lombardi C, Florio M, DeMarchi L and others (2016) An *in situ* assessment of local adaptation in a calcifying polychaete from a shallow CO_2 vent system. Evol Appl 9:1054–1071

Luppi T, Bas C, Méndez Casariego A, Albano M and others (2013) The influence of habitat, season and tidal regime in the activity of the intertidal crab *Neohelice* (=*Chasmagnathus*) *granulata.* Helgol Mar Res 67:1–15

Mat AM, Dunster GP, Sbragaglia V, Aguzzi J, de la Iglesia HO (2017) Influence of temperature on daily locomotor activity in the crab *Uca pugilator.* PLOS ONE 12: e0175403

Moriyama T, Enomoto K, Kawai H, Watanabe S (2017) Circatidal activity rhythms in the soldier crab *Mictyris guinotae.* Biol Rhythm Res 48:129–139

Nordhaus I, Diele K, Wolff M (2009) Activity patterns, feeding and burrowing behaviour of the crab *Ucides cordatus* (Ucididae) in a high intertidal mangrove forest in North Brazil. J Exp Mar Biol Ecol 374:104–112

Novak M (2004) Diurnal activity in a group of Gulf of Maine decapods. Crustaceana 77:603–620

Pombo M, Campagnoli M, Castilho-Martins EA, Turra A (2018) Continuous, video-recording assessment of daily activity cycle of the ghost crab *Ocypode quadrata* Fabricius, 1787 (Brachyura: Ocypodidae) in southeastern Brazil. J Crustac Biol 38:133–139

Reid DG, Naylor E (1989) Are there separate circatidal and circadian clocks in the shore crab *Carcinus maenas?* Mar Ecol Prog Ser 52:1–6

Saidi A, Banchi E, Fonti V, Manna V and others (2023) Microbial dynamics in shallow CO_2 seeps system off Panarea Island (Italy). Mar Biol 170:97

Shmuel Y, Ziv Y, Rinkevich B (2022) *Trapezia* crabs that dwell in distinctive day/night canopy compartments of a marine animal forest, forage on demersal plankton. J Mar Sci Eng 10:1522

Skajaa K, Fernö A, Løkkeborg S, Haugland EK (1998) Basic movement pattern and chemo-oriented search towards baited pots in edible crab (*Cancer pagurus* L.). Hydrobiologia 371:143–153

Styrishave B, Aagaard A, Andersen O (1999) *In situ* studies on physiology and behaviour in two colour forms of shore crabs *Carcinus maenas* in relation to season. Mar Ecol Prog Ser 189:221–231

Takahashi K, Kawaguchi K (2001) Nocturnal occurrence of the swimming crab *Ovalipes punctatus* in the swash zone of a sandy beach in northeastern Japan. Fish Bull 99: 510–515

Tunnicliffe V, Garrett JF, Johnson HP (1990) Physical and biological factors affecting the behaviour and mortality of hydrothermal vent tubeworms (vestimentiferans). Deep Sea Res A Oceanogr Res Pap 37:103–125

Voight JR (2000) A review of predators and predation at deep-sea hydrothermal vents. Cah Biol Mar 41: 155–166

Wang TW, Chan TY, Chan BKK (2014) Trophic relationships of hydrothermal vent and non-vent communities in the upper sublittoral and upper bathyal zones off Kueishan

Island, Taiwan: a combined morphological, gut content analysis and stable isotope approach. Mar Biol 161: 2447–2463

Wang TW, Lau DCP, Chan TY, Chan BKK (2022) Autochthony and isotopic niches of benthic fauna at shallow-water hydrothermal vents. Sci Rep 12:6248

Wang YV, Larsen T, Lebrato M, Tseng LC and others (2023) Foraging under extreme events: contrasting adaptations by benthic macrofauna to drastic biogeochemical disturbance. Funct Ecol 37:1390–1406

Wu JY, Lin SY, Peng SH, Hung JJ, Chen CTA, Liu LL (2021) Isotopic niche differentiation in benthic consumers from shallow-water hydrothermal vents and nearby non-vent rocky reefs in northeastern Taiwan. Prog Oceanogr 195: 102596

Yang CH, Wang TW, Ng PKL, Chan TY, Lin YY, Chan BKK (2022) Population genetic differentiation on the hydrothermal vent crabs *Xenograpsus testudinatus* along depth and geographical gradients in the Western Pacific. Diversity 14:162

Zeng C, Abello P, Naylor E (1999) Endogenous tidal and semilunar moulting rhythms in early juvenile shore crabs *Carcinus maenas*: implications for adaptation to a high intertidal habitat. Mar Ecol Prog Ser 191:257–266

Editorial responsibility: Antony Underwood, Sydney, New South Wales, Australia
Reviewed by: T. Moriyama, M. Pombo, J. Hall-Spencer

Submitted: March 18, 2024
Accepted: July 22, 2024
Proofs received from author(s): August 31, 2024